Heating and Non-inductive Current Drive by Negative-ion based NBI in JT-60U

T. OIKAWA, K. USHIGUSA, C. B. FOREST[1], M. NEMOTO, O. NAITO, Y. KUSAMA, Y. KAMADA, K. TOBITA, S. SUZUKI, T. FUJITA, H. SHIRAI, T. FUKUDA, M. KURIYAMA, T. ITOH, Y. OKUMURA, K. WATANABE, L. GRISHAM[2] and THE JT-60 TEAM

Japan Atomic Energy Research Institute, Naka Fusion Research Establishment, Naka-machi, Naka-gun, Ibaraki-ken, Japan

[1] University of Wisconsin-Madison

[2] Princeton Plasma Physics Laboratory

ABSTRACT

Current drive and heating properties of negative-ion-based NBI(N-NBI) have been studied comprehensively in JT-60U. It was confirmed from the shinethrough measurements of the injected beam(350keV) that multi-step ionization processes are essential in the ionization processes of high energy particles. A current density profile driven by N-NB was determined experimentally. That is in a good agreement with theoretical prediction, and N-NB driven current reached 0.6MA with E_B=360keV and P_{INJ}=3.7MW. Current drive efficiency η_{CD} is increased with the electron temperature and improved with beam energy. Injected fast ions are well confined in the enhanced confinement core with weak poloidal magnetic field of the reversed shear plasmas. Clear H-mode transition was obtained with N-NB dominant heating, where the net absorbed power required for H-mode transition seemed similar to the previous result obtained in JT-60U using positive-ion-based NBI(P-NBI) heating. With the strong electron heating by N-NB (80% absorbed by the electron), H factor ($=\tau_E/\tau_E^{ITER89PL}$) of 1.64 with $T_e(0)=1.4T_i(0)$ was obtained in the steady-state ELMy phase.

1. INTRODUCTION

Heating and current-drive are important issues for steady-state operation in the tokamak fusion reactor with high density and temperature core plasma. Neutral beam injection(NBI) is one of the most promising candidates for these purposes because of its applicability established in the tokamak experiments with successful results of the current drive of several hundreds of kA ~ 1MA level and the improved confinement. In the reactor plasmas, beam energy of MeV class is required to penetrate deeply into the high density core. Negative-ion based NBI(N-NBI) has a much higher neutralization efficiency at high beam energy over several hundreds of keV comapred to positive-ion based NBI(P-NBI), which has been used in many tokamaks. Thus, N-NBI system has to be establishd technologically and prove to be applicable and effective for heating and current drive in tokamak plasmas. JT-60U's N-NBI system has been installed in 1996[1]. It is a co-directional tangential beam consisting of two beam-lines(NNB-U and NNB-L) as shown in Fig. 1 and has the designed values of beam energy E_B=500keV, injection power P_{INJ}=10MW and pulse length of 10s[2]. High production efficiency of negative-ions and high neutralization efficiency were confirmed in the range of 300-400keV. By solving the engineering problems accompanying the high-voltage acceleration of negative ion beam at high-power for long duration, E_B up to 400keV, P_{INJ} up to 5.2MW and duration time of 1.9s have been achieved[3]. The experiments using N-NBI have been conducted extensively in the various aspects. In this paper, the ionization process as a basis of power absorption, current drive performance, confinement of N-NB fast ions and N-NB H-mode are described.

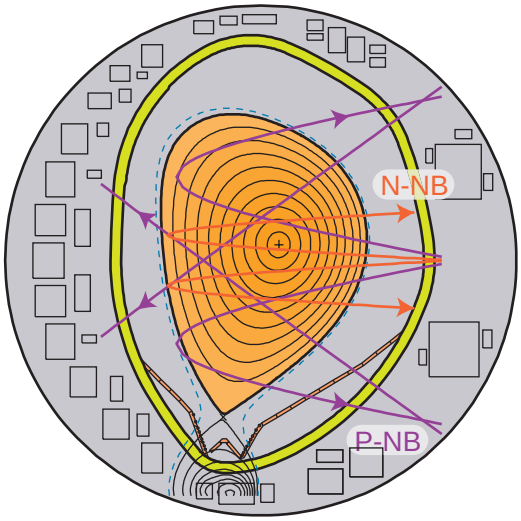

Fig. 1. Plasma configuration. N-NB trajectories projected on the poloidal plane are shown.Upper line is called NNB-L(injected from the lower ion-source placed below the equatorial-plane of the torus), and Lower line is NNB-U injected from the upper ion source. Trajectories of tangential and perpendicular P-NB are also shown. Magnetic surfaces are shown by normalized minor radius.

2. IONIZATION PROCESS OF N-NBI HIGH ENERGY PARTICLES

The multi-step ionization[4], which arises from excitation processes of the beams and the subsequent ionization, can be important in neutral beams with energies of several hundreds of keV or higher. The cross-section for electron loss(ionization and charge exchange) can be enhanced through the multi-step processes, and it is predicted theoretically that the enhancement factor δ is increased with raising E_B and n_e. Here, the enhancement factor is defined by $\delta = (\sigma_{multi} - \sigma_{single}) / \sigma_{single}$, where σ_{multi} and σ_{single} are cross-sections for multi- and single-step models respectively. From calculation of the multi-step model by Janev[4], δ can be as large as 20% when E_B=500keV and $n_e=1\times10^{19}m^{-3}$ in hydrogen plasma. Fig. 2(a) shows N-NB(E_B=355keV, P_{NNB}=3MW) power deposition profiles calculated by OFMC[5] code using single- and multi-step models. Plasma parameters are $\bar{n}_e=1\times10^{19}m^{-3}$, $T_e(0)$=4.2keV, $T_i(0)$=3keV and Z_{eff}=2.8. Deposition profiles are quite different even with relatively-low density. Total absorbed powers for two models are 1.3 and 2.2MW, respectively. Thus, the beam stopping cross-section has a large impact on the estimation of beam deposition. To validate theoretical predictions on the multi-step ionization for reliable design of N-NBI with MeV-class beam energy requested on the reactor, cross-section should be evaluated experimentally in the high energy range. The experimental data obtained so far was up to 140keV[6] at which difference between single- and multi-step models was not large and it is difficult to confirm the multi-step model experimentally.

Ionization process of N-NBI has been studied experimentally from shine-through measurements[7], where both plasma and beam species are hydrogen. The shine-through is estimated from the temperature rise of armor tiles facing the N-NB lines using thermocouples. In this series of experiments, the ranges of T_e and Z_{eff} are 1.8 - 3.7keV and 1.3 - 2.2, respectively. Fig. 2(b) shows dependence of measured shine-through of 350keV N-NBI on n_eL, where n_eL is the integrated electron density along the beam path in the plasma. Two theoretical predictions, single- and multi-step ionization processes, are also shown in the Fig. 2(b) (shaded areas). Here, on comparing the experimental results to the theoretical calculation, cross-section for electron loss due to multi-step processes is newly calculated by adopting the latest reliable atomic data[8] based on the work by Janev *et al.*[4]. Experimental results agree with multi-step processes over a wide range of n_eL ($0.7\text{-}3.0\times10^{20}m^{-2}$ corresponding to $\bar{n}_e=1\text{-}4.1\times10^{19}m^{-3}$) within the experimental error due to 20% uncertainty in Z_{eff}. Multi-step ionization processes are essential in high E_B and n_e regime. Fig. 2(c) shows n_eL dependence of the enhancement factor δ. Theoretical results mentioned above are also shown(open circles). Here, as it is a line-averaged value of δ that can be evaluated from shinethrough measurement, theoretical δ compared in Fig. 2(c) are also averaged from δ profile along the beam path. Enhancement has the value of 0.3 at $n_eL=2\times10^{20}m^{-2}$($\bar{n}_e=3\times10^{19}m^{-3}$), increasing gradually with the density.

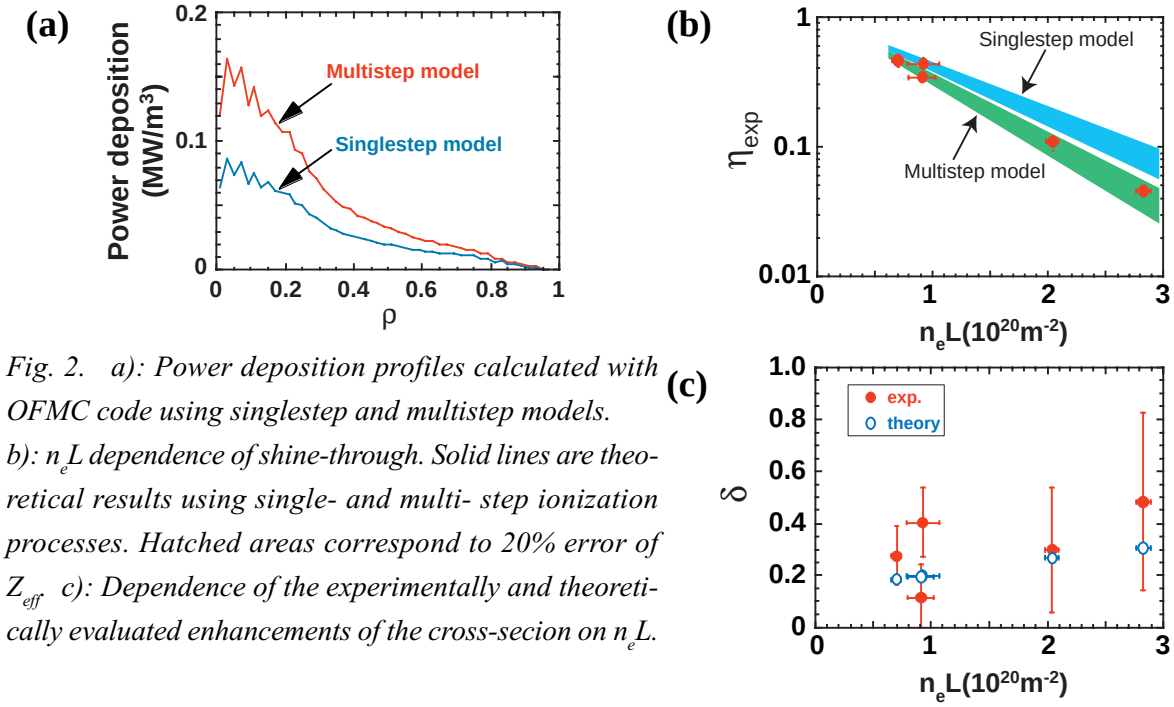

Fig. 2. a): Power deposition profiles calculated with OFMC code using singlestep and multistep models. b): n_eL dependence of shine-through. Solid lines are theoretical results using single- and multi- step ionization processes. Hatched areas correspond to 20% error of Z_{eff} c): Dependence of the experimentally and theoretically evaluated enhancements of the cross-secion on n_eL.

Our theoretical work[8] also takes into account the case when characteristic length for saturation of excitation probability can't be negligible compared to the mean free path for electron loss of beam neutrals, which correponds to the effect of the spatial distribution of density and temperature. Calculated result shows that the effect of the spatial distribution of n_e and T_e become important at order of $n_e=10^{22}m^{-3}$. Thus, the conventional treatment of the population of each excited states to be saturated can be applicable to the high beam energy and density in the fusion reactors.

3. N-NB CURRENT DRIVE

N-NB current drive experiments with deuterium plasma and beam have been carried out to make clear current drive properties of N-NBI, which is a basis in application of N-NBI to sustainment of high

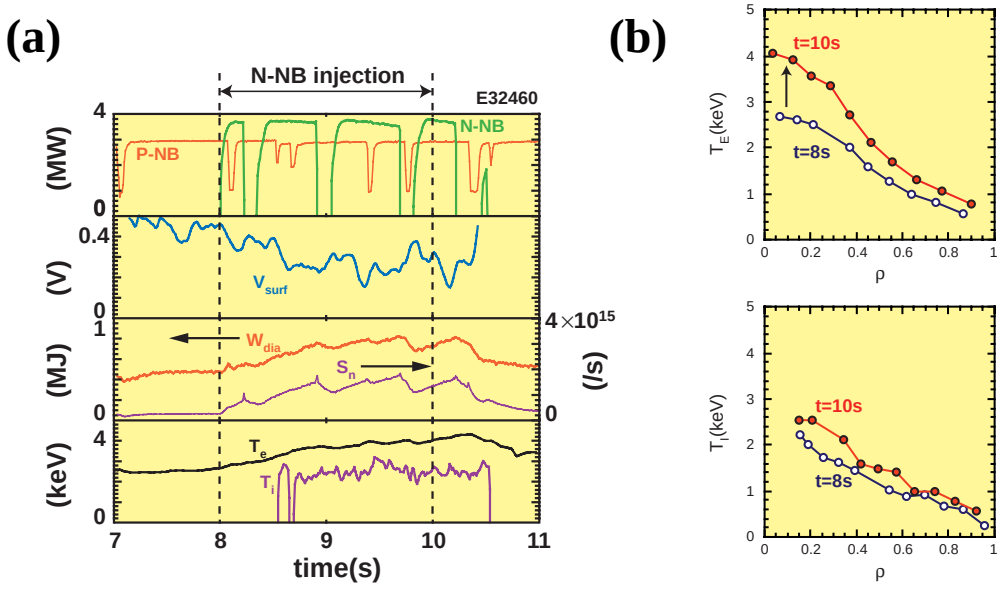

Fig. 3. a): Waveforms of N-NBCD experiment. During N-NB injection, drop of V_{surf}, increases in W_{dia} and S_n are observed. $T_e(0)$ also increases, while increase in $T_i(0)$ is small. b): T_e and T_i profile before and during N-NB injection, which indicates electron dominant heating by N-NB.

performance discharges with full current drive. Profile of loop voltage has to be determined to evaluate N-NB driven current profile $j_{NNB}(\rho)$ and total driven current I_{NNB}. Non-inductive portion of current is the difference between the total current density $j(\rho)$ and the inductive current density $j_{oh}(\rho)$. Total current density profilie $j(\rho)$ is determined accurately from equilibrium reconstruction[9] with external magnetic measurements and internal Motional Stark Effect(MSE) measurements[10], and $j_{oh}(\rho)$ can be determined from the internal electric-field(loop voltage) profile $E_{//}(\rho)$ and the resistivity profile calculated from measured $T_e(\rho)$, $n_e(\rho)$ and $Z_{eff}(\rho)$ based neo-classical conductivity(confirmed in JT-60[11]), where $E_{//}(\rho)$ is calculated from time-evolution of poloidal flux profile $\Psi(\rho)$[12].

Plasma configuration(Fig. 1) is chosen as MSE and Thomson scattering measurements can cover from the magnetic axis to the edge to reconstruct equilibrium and determine resistivity profile with high accuracy because the accuracies of measurements are quite important in the analysis method mentioned above. Lower unit of N-NB passes through the magnetic axis in this configuration. Fig. 3(a) shows NB power and plasma parameters at I_P=1MA, B_T=3.5T and $\bar{n}_e=0.9\times10^{19}m^{-3}$. N-NB injection power is 3.7MW at E_B=360keV. Pulse length (>2s) is sufficiently longer than the slowing down time of N-NB fast ions, 0.5 - 0.65s inside half minor radius where 60% of N-NB inection power is absorbed. P-NB of 3MW is also injected for measurements of current density and ion temperature T_i profiles using MSE and Charge Exchange Recombination Spectroscopy(CXRS), respectively. Stored energy, W_{dia}, and neutron emission rate, S_n, increase during N-NB injection. The large increase in S_n is mostly due to beam-thermal reaction. Central electron temperature $T_e(0)$ increases during N-NB injection, while increase in ion temperature $T_i(0)$ is small(Fig. 3(a)). Electron and ion temperature profiles before and during N-NB injection are shown in Fig. 3(b). These indicate electron dominant heating by N-NBI with central deposition($T_e(0)$~4keV, $T_i(0)$~2.7keV). From calculation of OFMC code, absorbed power in electrons and ions during slowing-

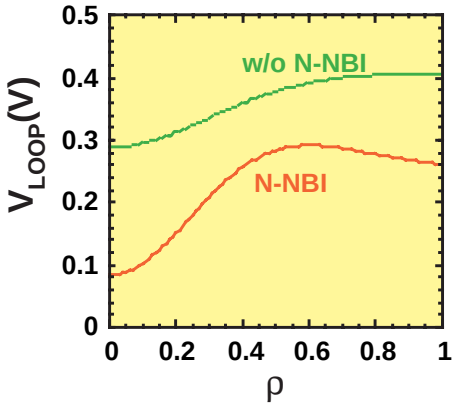

Fig. 4 *: Loop voltage profiles with and without N-NB injection. Large drop in the central region is observed in case of N-NB injection.*

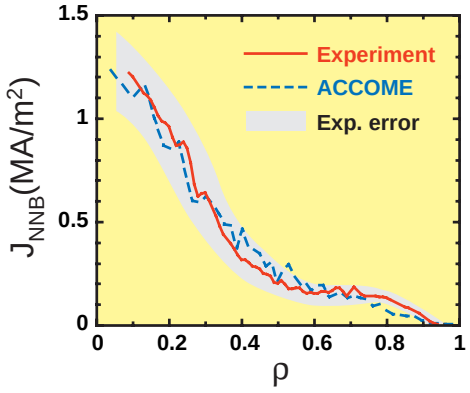

Fig. 5 *: N-NB driven current profile. Experimental result(solid line) agrees well with theoretical calculation(dashed line). Error bar due to the uncertainties in T_e, Z_{eff} and V_{loop} is indicated by shaded region.*

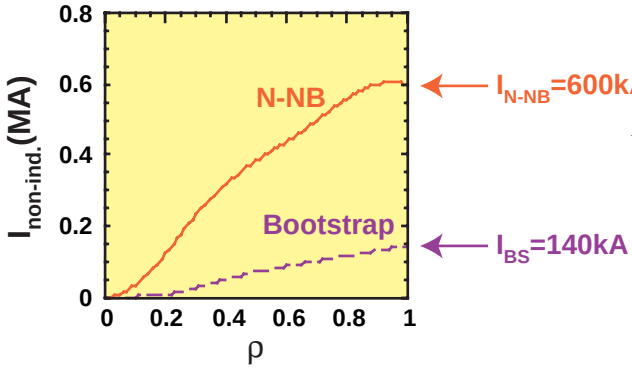

Fig. 6 *: Integrated N-NB driven and bootstrap currents inside each flux surface versus normalized minor radius ρ. Total N-NB driven current is 600kA and Bootstrap current is 140kA.*

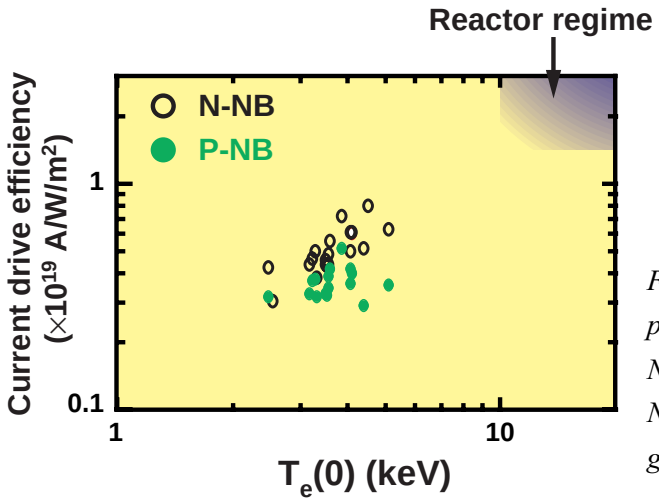

Fig. 7. Central electron temperature $T_e(0)$ dependence of current drive efficiency η_{CD} for N-NB(open circles) of E_B=330-370keV and for P-NB(closed circles) of E_B=83-87keV. Shaded region indicates the required regime for reactor.

down process of N-NB fast ions are 61% and 14% of injection power, respectively. 26 and 35% of injected P-NB power go to electrons and ions, respectively. Shinethrough loss is 21% for N-NB and 19% for P-NB and other losses due to toroidal field ripple, banana drift orbit and charge exchange are 4% for N-NB and 20% for P-NB. Electron density almost stays at constant level because of low particle fueling of N-NBI. Gradual decrease in surface voltage V_{surf} from 0.45V to less than 0.3V is due to the gradual T_e increase and relaxation of electric field(loop voltage profile becomes flat).

Loop voltage profiles at the same timing of discharges with and without N-NB injection are shown in Fig. 4. Large drop of loop voltage in the central region is observed. This is due to reductions of the inductive current density and resistivity through increase in electron temperature by N-NB central current-drive and heating. N-NB driven current density profile $j_{NNB}(\rho)$ is evaluated by the technique mentioned above. This analysis method gives just non-inductive portion of current profile and can't separate beam-driven and bootstrap components. Thus, $j_{NNB}(\rho)$ is determined by subtracting bootstrap current profile $j_{BS}(\rho)$ calculated by the theoretical code from non-inductive current profile. N-NB driven current profile is shown in Fig. 5 (solid line). The centrally-peaked profile is confirmed experimentally as expected from on-axis trajectory of N-NB. Total N-NB driven current I_{NNB} is 600kA and the current-drive efficiency η_{CD} defined by $\eta_{CD} = \bar{n}_e R_P I_{NNB} / P_{INJ}(1-\eta_{SHT})$ is $0.6\times10^{19}AW^{-1}m^{-2}$, where η_{SHT} is a shinethrough fraction. A calculated $j_{NNB}(\rho)$ using current-drive code ACCOME[13] is also shown (dashed line). They agree well within the experimental error due to the uncertainties in T_e, Z_{eff} and loop voltage. Fig. 6 shows the integrated N-NB driven and bootstrap currents inside each ρ for the same discharge in Fig. 3-5. 70% of I_{NNB} is driven insid half minor radius. Bootstrap current I_{BS} is 140kA, where contribution of NNB to fast-ion component of I_{BS} is calculated as ~50kA.

Fig. 7 shows η_{CD} as a function of $T_e(0)$ for N-NBI(E_B=330-370keV) and P-NB(E_B=83-87keV). Electron temperature is 2-6 keV, and Z_{eff} is 2-3.5. They are obtained in the same series of N-NB current drive experiments. Current drive efficiency increases with $T_e(0)$. Central value is chosen as a representative value characterizing η_{CD} because N-NB has a central deposition. Increase in η_{CD} with higher T_e is due to longer slowing down time of beam ions. Fig. 7 also shows that η_{CD} is improved with beam energy(higher η_{CD} for N-NB than that for P-NB). These result of increase in current drive efficiency with T_e and beam energy, which is predicted by theory, indicate that current-drive performance of neutral beam can reach the value required for the fusion reactor with beam energy~1MeV, T_e>10keV and Z_{eff}~1.5.

4. Confinement of N-NBI high energy ions

As is shown in recent experimental results in tokamak devices[14,15], a reversed magnetic shear (R/S) plasma with internal transport barriers (ITBs) is the most promising candidate for an advanced steady state operation of a tokamak reactor. However, loss of high energy trapped particles can be en-

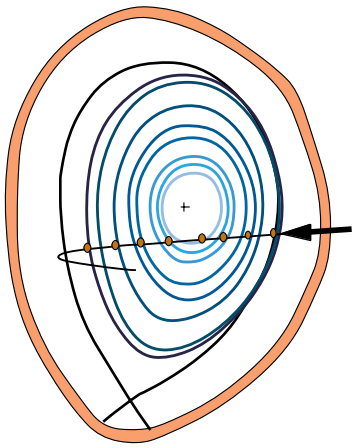

Fig. 8. First orbit of N-NB fast ions in the reversed shear plasma. Most of fast ions are initially produced in passing orbits.

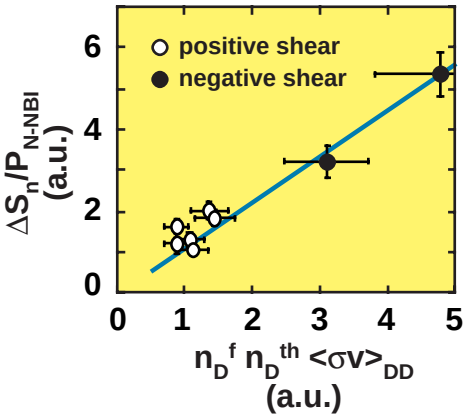

Fig. 9. The ratio of measured increase in neutron emission to calculated one is constant, which means confinement of N-NB fast ions is not degraded in negative sheaer with weak poloidal magnetic field.

hanced due to ripple transport, especially in the reversed shear plasmas because the banana-width becomes large in the negative shear region due to the small poloidal magnetic field. N-NB fast ions are expected to be confined well in the plasma without suffering ripple transport because most of them are initially produced in passing orbits as shown in Fig. 8(calculated result). Fig. 9 shows increases in neutron emission by N-NB injection into positive and negative magnetic shear plasmas as a function of the values calculated from T_e and Z_{eff}. Values of $\Delta S_n/P_{NNB}$ in positive (open circles) and negative (closed circles) shear plasmas are on the same line. This means that N-NBI fast ions are well confined even in a weak poloidal magnetic field of reversed shear plasmas. Thus, N-NB fast ions heat plasma effectively during slow-down process. Fig. 9 also means that the effect of deviation of passing fast ion from magnetic surface is small. This is because deviation(order of poloidal larmor radius) is small compared with the scale length of plasma profiles such as temperature, and the outer and inner shifts of drift surface respectively in low and high field side cancel each other. Thus, this effect doesn't affect current drive calculation much(ACCOME code assumes fast ions running on the magnetic surface).

5. N-NB H-mode

Considering N-NBI as a main heating tool for reactor plasmas, it is quite important to confirm H-mode transition with N-NBI. As shown in Fig. 10(a), clear H-mode transition occurs at t=6.1s during N-NB injection of 3.89MW at E_B=336keV. In this discharge, the injected power of P-NB for diagnostic is 0.8MW. Fig. 10(b) shows T_e and T_i profiles at 1s after H-mode transition for similar discharge. Electron temperature is higher than T_i, especially over 1.4 times in the center, due to the electron dominant heating by N-NBI as calculation of OFMC code shows that the absorbed power in electrons is 5 times larger than that in ions. Threshold power predicted by the scaling $P^{TH}(MW)=1.1\bar{n}_e^{0.5}[10^{19}m^{-3}]B_T^{1.0}[T]$ obtained in JT-60U using P-NB[16, 17] is 2.6MW at B_T=2.05T and the target density $\bar{n}_e=1.34\times10^{19}m^{-3}$ in this discharge. The absorbed P-NB power P_{abs}^{PNB} and ohmic input P_{OH} are 0.75MW(4% of shinethrough is subtracted from the injection power) and 0.68MW, respectively. As the sum of these are below threshold power 2.6MW, the observed H-mode transition is kicked by N-NB injection. At the H-mode transition, the net absorbed power $P_{net}(\equiv P_{abs}^{NNB}+P_{abs}^{PNB}+P_{OH}-dW_{ST}/dt)$ is 3.53MW(shinethrough losses of 26%(N-NB) and 4%(P-NB) are subtracted).

In the steady-state ELMy phase(t=7.44s), H-factor(ITER-89PL) is 1.64. ELMy H-mode is sustained over 1.3s, which is longer than the slowing-down time of N-NB fast ions(0.27s in the center). It

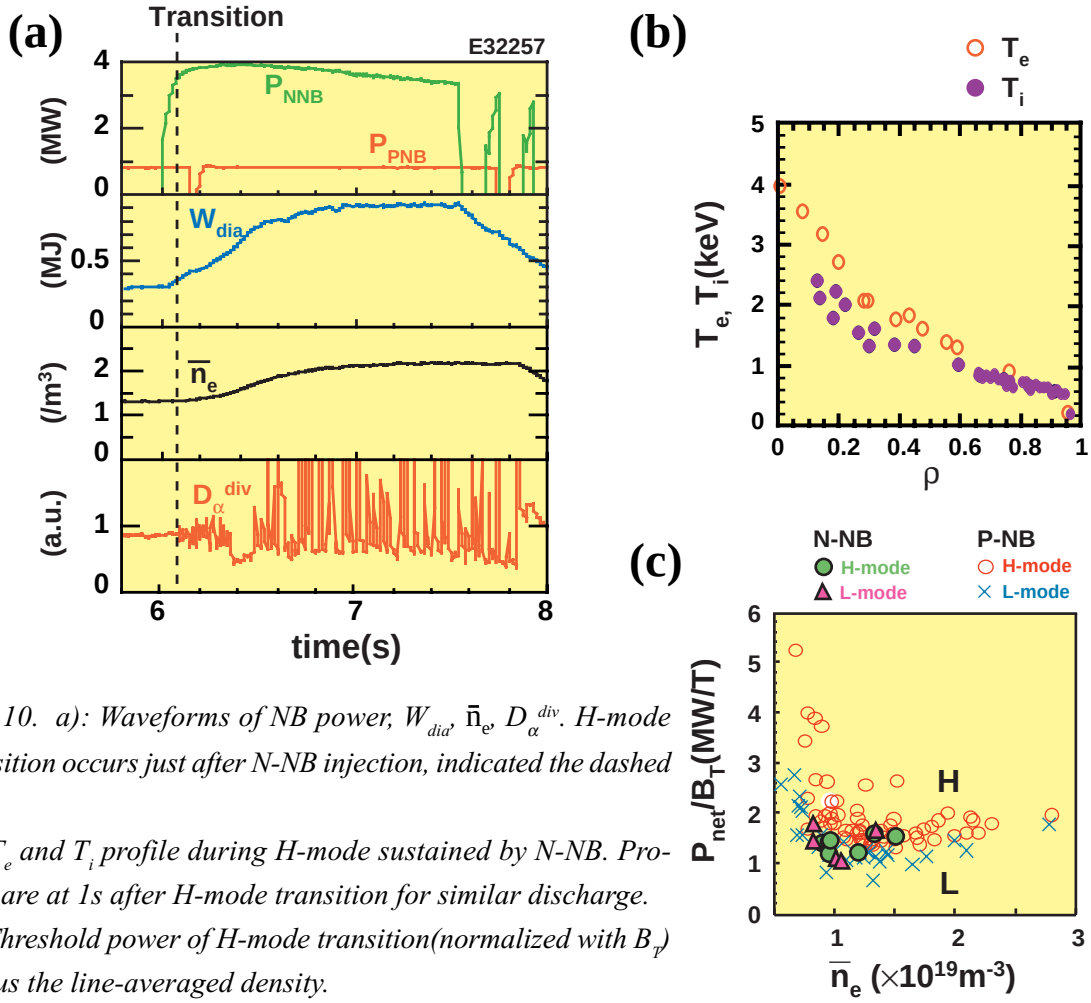

Fig. 10. a): Waveforms of NB power, W_{dia}, $\bar{n}_e$, D_α^{div}. H-mode transition occurs just after N-NB injection, indicated the dashed line.
b): T_e and T_i profile during H-mode sustained by N-NB. Profiles are at 1s after H-mode transition for similar discharge.
c): Threshold power of H-mode transition(normalized with B_T) versus the line-averaged density.

should be noted that this H-factor of 1.64, which is almost the same as that obtained by P-NB heating at $T_e \sim T_i$ in JT-60U, can be obtained at $T_e > T_i$.

In Fig. 10(c), the net absorbed power normalized with toroidal field is plotted as a function of $\bar{n}_e$. H- and L-modes with P-NB heating are indicated by open circles and crosses, respectively. Those with N-NB and P-NB heating, where the fractions of P_{INJ}^{NNB} to the total injection power are 40-100%, are indicated by closed circles and triangles, respectively. In the low density region ($\bar{n}_e < 1.2\times10^{19}m^{-3}$), threshold power increases with decreasing density, which is same as for P-NB. This is because the ratio of edge neutral density n_0 and n_e increases in this range of density and threshold power is largely affected by edge neutrals[17,18]. It seems that H-mode transition by N-NBI occurs at similar level to P-NB heating within the present N-NB H-mode data restricted in the narrow range of parameters such as B_T, $\bar{n}_e$ and q_{eff}. Further detailed and systematic experiments is necessary to conclude whether the threshold power scaling with N-NB is different from that with P-NB ($P^{TH}(MW) = 1.1\bar{n}_e^{0.5}[10^{19}m^{-3}]B_T^{1.0}[T]$ for $\bar{n}_e > 1.2\times10^{19}m^{-3}$).

6. SUMMARY

In JT-60U, issues related with high energy neutral beam have been studied comprehensively. On the basis of plasma heating and current drive, the ionization processes of high energy particles are examined both experimentally and theoretically. These make clear the multi-step ionization processes involving the excited states are essential in high beam energy and density region. Current drive properties , e.g., non-inductively driven current profile and total driven current, are evaluated from measurements, which show good agreement with the theoretical prediction. Current drive efficiency is found to be increased

with the electron temperature and improved with the beam energy. These results give the prospect that current-current drive performance required for the fusion reactor can be achieved with neutral beam. N-NB fast ions are well confined in the reversed shear plasma and can heat the improved confinement core in the slowing down process without suffering ripple transport. Clear H-mode transition is obtained by N-NB dominant heating with H-factor of 1.64 at $T_e > T_i$. This good confinement with $T_e > T_i$ is a new regime in JT-60U, which has been achieved by N-NBI. H-mode transition power doesn't deviate from the scaling obtained in the previous JT-60U experiments, although detailed and systematic experiments are necessary for H-mode properties and physics such as threshold power, pedestal behaviours and the effects of the pure electron heating and high energy ions.

As for the progress on JT-60U's N-NBI, E_B=400keV, P_{INJ}=5.2MW and pulse duration of 1.9s have been achieved. Next step with progress on N-NBI system is furthur improvement of high performance plasmas through current profile and pressure profile optimization with high fraction of non-inductive current using N-NBI.

ACKNOWLEDGMENTS

The authors would like to acknowledge Drs. L. L. Lao and T. S. Taylor in General Atomics for the corporation of equilibrium-code supporting current-drive study in JT-60U. They would like to thank the members of the Japan Atomic Energy Research Institute who have contributed to the JT-60U project. They also express their gratitude to Drs. H. Kishimoto, M. Azumi, M. Kikuchi and T. Takizuka for fruitful discussion, continuous support and encouragement.

REFERENCES

[1] Ushigusa, K., *et al*., Fusion Energy Proc. 16th Int. Conf. (Montreal, 1996), IAEA, Vol.1, Vienna(1997)37.

[2] Kuriyama, M., *et al.*, Fusion Engineering and Design, **26**(1995)445.

[3] Kuriyama, M., *et al.*, Proc. 20th Symposium on Fusion Technology, vol.1 (1998)391.

[4] Janev, R. K., *et al*., Nuclear Fusion **29**(1989)2125.

[5] Tani, K., *et al*., Journal of Phys. Soc. Jpn. **50** (1981)1726.

[6] Tobita, K., *et al*., Plasma Phys. Controlled Fusion **32**(1990)429.

[7] Nemoto, M., *et al*., Journal of Plasma and Fusion Research **73**(1997)1374.

[8] Suzuki, S., *et al*., Plasma Phys. Controlled Fusion (in press).

[9] Lao, L. L., *et al*., Nuclear Fusion **20** (1990)1025.

[10] Fujita, T., *et al*., Fusion Engineering and Design, **34-35**(1995)282.

[11] Kikuchi, M., *et al*., Nuclear Fusion **29** (1990)343.

[12] Forest, C. B., *et al*., Phys. Rev. Lett. **73** (1994)2444.

[13] Tani, K., Azumi, M., Journal of Computational Physics **98** (1992)332.

[14] Fujita, T., *et al*., Phys. Rev. Lett. **78** (1997)2377.

[15] Fujita, T., *et al*., IAEA-CN-69/EX1/2, this volume.

[16] Sato, M., *et al*., Plasma Phys. Controlled Fusion **38** (1996) 1283.

[17] Fukuda, T., *et al*., Proc. of 16th IAEA Fusion Energy Conference(IAEA, Vienna) 1996.

[18] Tsuchiya, K., *et al*., Plasma Phys. Controlled Fusion **38**(1996)1295.